

Heterogeneous & Homogeneous & Bio- & Nano-

CHEM **CAT** CHEM

CATALYSIS

Accepted Article

Title: 2D-2D Nanocomposite of MoS₂-Graphitic Carbon Nitride as Multifunctional Catalyst for Sustainable Synthesis of 3C-functionalized Indoles

Authors: Ashish Bahuguna, Ashwani Kumar, Suneel Kumar, Tripti Chhabra, and Venkata Krishnan

This manuscript has been accepted after peer review and appears as an Accepted Article online prior to editing, proofing, and formal publication of the final Version of Record (VoR). This work is currently citable by using the Digital Object Identifier (DOI) given below. The VoR will be published online in Early View as soon as possible and may be different to this Accepted Article as a result of editing. Readers should obtain the VoR from the journal website shown below when it is published to ensure accuracy of information. The authors are responsible for the content of this Accepted Article.

To be cited as: *ChemCatChem* 10.1002/cctc.201800369

Link to VoR: <http://dx.doi.org/10.1002/cctc.201800369>

2D-2D Nanocomposite of MoS₂-Graphitic Carbon Nitride as Multifunctional Catalyst for Sustainable Synthesis of 3C-functionalized Indoles

Ashish Bahuguna, Ashwani Kumar, Suneel Kumar, Tripti Chhabra and Venkata Krishnan*

School of Basic Sciences and Advanced Materials Research Center, Indian Institute of Technology Mandi, Kamand, Himachal Pradesh 175005, India.

Email: vkn@iitmandi.ac.in

Abstract

A nanocomposite of two dimensional MoS₂ supported on gC₃N₄ nanosheets has been prepared by a facile ultrasonication method followed by demonstrating its ability to catalyze the synthesis of several indole derivatives. The as-prepared nanocomposite catalyst was characterized in detail using different microscopic and spectroscopic techniques to understand its structure and physico-chemical properties. Subsequently, this nanocomposite catalyst was used as a heterogeneous multifunctional catalyst to synthesize several 3C-functionalized indoles in the aqueous medium. The employed strategy also provided very good catalyst recyclability and versatility for the synthesis of various precursors of medicinally significant indoles, such as serotonin, melatonin and various beta-carboline alkaloids. In addition, a natural product derivate has been prepared in gram-scale using this methodology. Furthermore, high atom economy (100%) and lower E-factor (0.042) makes this strategy a sustainable approach for the synthesis of 3C-functionalized indoles.

Keywords: Two dimensional material; nanocomposite; multifunctional catalyst; sustainable synthesis; functionalized indoles

Introduction

Catalysis and catalytic processes, such as homogeneous and heterogeneous processes, are involved in all the major chemical production of the world.¹ Traditional heterogeneous catalysts have been found to be comparatively low active due to limited or less accessibility of the reagents to the active sites of the catalysts. A catalyst support material can overcome this problem by supporting the active sites on different other porous inorganic solids, such as zeolite,^{2, 3} silica⁴⁻⁶ and various other mesoporous or even organic polymeric materials.^{4, 7-9} Therefore, selection of an appropriate catalytic support is of utmost importance.

Carbon and carbonaceous materials play a very significant role in catalysis, either as a catalyst or a catalyst support for various chemical, biological and enzymatic transformation reactions. There are several advantages of these materials due to their large surface area, excellent electron conductivity, high porosity and relatively chemical inertness in mild reaction conditions. Metal catalysts on carbon supports have various advantages over other catalytic materials for various types of reactions.¹⁰⁻¹³ The future success of catalysis demands to design new kinds of multifunctional catalytic materials possibly emerging from carbonaceous materials, such as charcoal,^{14, 15} carbon nanotubes,^{16, 17} carbon fibers,^{18, 19} carbon aerogels,²⁰ graphene,^{21, 22} graphitic carbon nitride(GCN),^{23, 24} etc. Activated carbon^{25, 26} and carbon black^{27, 28} have been preferred choices of the materials among the carbon-supported catalysts due to their high surface area, low cost and easy availability in large quantities. In the recent decade, carbon materials, such as graphitic materials and activated carbons have been extensively used in heterogeneous catalysis as catalyst supports.²⁹⁻³¹ The physiochemical properties of these materials, such as their mechanical strength, tunable porosity, chemical/ thermal stability and surface chemistry make them suitable for many catalytic application processes.

In recent years, organic transformations using the environmentally benign(Green) approaches of synthesis and sustainable methods are in demand from industries and society.³² Among several Green methods of synthesis, nanocomposite catalyzed organic transformations has drawn significant attention from a wide range of researchers working in different fields of chemistry.^{33, 34} Organic transformations using nanocomposites has several advantages, such as

simple filtration due to heterogeneous nature, easy to handle, efficient recovery and reusability of catalyst, etc. Minimization of waste leads to higher atom economy and lower E-factor play significant role in Green and sustainable chemistry. Moreover, nanocomposite catalyzed reaction with two dimensional (2D) metal dichalcogenides^{35, 36} such as, MoS₂ has attracted much attention recently. In addition to its wide application in material chemistry, MoS₂ is now becoming one of the preferred choices for synthetic chemists as well, due to its large surface area and 2D nature. There are several examples available in the literature based on composites of different materials with MoS₂ such as MoS₂-ZnO, MoS₂-graphene, MoS₂-reduced graphene oxide (RGO) and MoS₂-GCN with varying surface area due to the difference in their interfacial contact with each other. MoS₂-RGO and MoS₂-GCN, due to 2D-2D nature have larger surface areas among several other composites. Graphitic carbon nitride (GCN) is a recently evolving material having unique structure and properties such as, 2D structure, good chemical stability, tunable electronic property and slight basic character due to nitrogen richness, which makes it suitable catalyst or catalyst support for various organic transformation reactions such as, oxidation,³⁷ hydrogenation,³⁸ activation of benzene,³⁹ acetylene hydrochlorination,⁴⁰ Knoevenagel condensation reactions,⁴¹ cyclisation of nitriles and alkynes,⁴² copper catalyzed azide-alkyne cycloaddition⁴³ and so on. In all these organic transformation reactions GCN either acts as a base or as a catalyst support.

MoS₂ based nanocomposites have shown their potential for some of the organic transformation reactions recently. Zhang et al. reported Mo over GO-Fe₃O₄ as an efficient catalyst for synthesis of spiro-oxindole scaffolds.⁴⁴ Wang et al. reported MoS₂-TiO₂ nanocomposite for thiocyanation of indoles.⁴⁵ In addition, our group has also developed nanocomposite of MoS₂-RGO as Green catalyst for one-pot synthesis of indole alkaloids.⁴⁶ Although several metal oxide and sulfides have been integrated with GCN for photocatalytic applications,^{47, 48} there are only limited reports on metal oxide and sulfide-based nanocomposites for the synthesis of indoles and their derivatives. 3C-substituted indole derivatives have drawn a lot of attention of synthetic chemists due to their vast applications as building blocks for several biologically active molecules. Various medicinally significant 3-substituted indoles such as, serotonin, melatonin, tryptamine, tryptophan, etc. are some of the

important key examples, whose chemical structures are shown in Figure 1. In addition, these 3C-functionalized indoles are the precursor to various natural products such as indoles alkaloids, beta-carboline alkaloids and various potent drugs as well⁴⁹⁻⁵¹. Yonemitsu et al. were the first to report one-pot synthesis of 3-substituted indoles using aldehydes, indoles and Maldrum's acid.⁵² Recently, Gu et al. reported Yonemitsu reaction for synthesis of 3-substituted indoles using aldehydes, indole, and dimedone in the presence of L-proline as a homogeneous catalyst.⁵³ Recently, Rawat et al. reported a heterogeneous ZnO-RGO nanocomposite for the synthesis of 3-substituted indole using aldehydes, indoles and a secondary amine.⁵⁴ Inspired by our continuous effort towards Green and sustainable synthesis, herein we report MoS₂-GCN nanocomposite catalyzed synthesis of 3C-functionalized indole derivatives of nitro alkenes and isatins. The proposed method is a mild, Green and very efficient method for the synthesis of various 3C-substituted indole derivatives. All the reactions have been carried out using the universal Green solvent, water. Due to the absence of by-products in the developed protocol and carrying out reactions in aqueous medium provide high value of atom economy (99%) and low E-factor (0.04), which are essential parameters for a sustainable synthetic method.

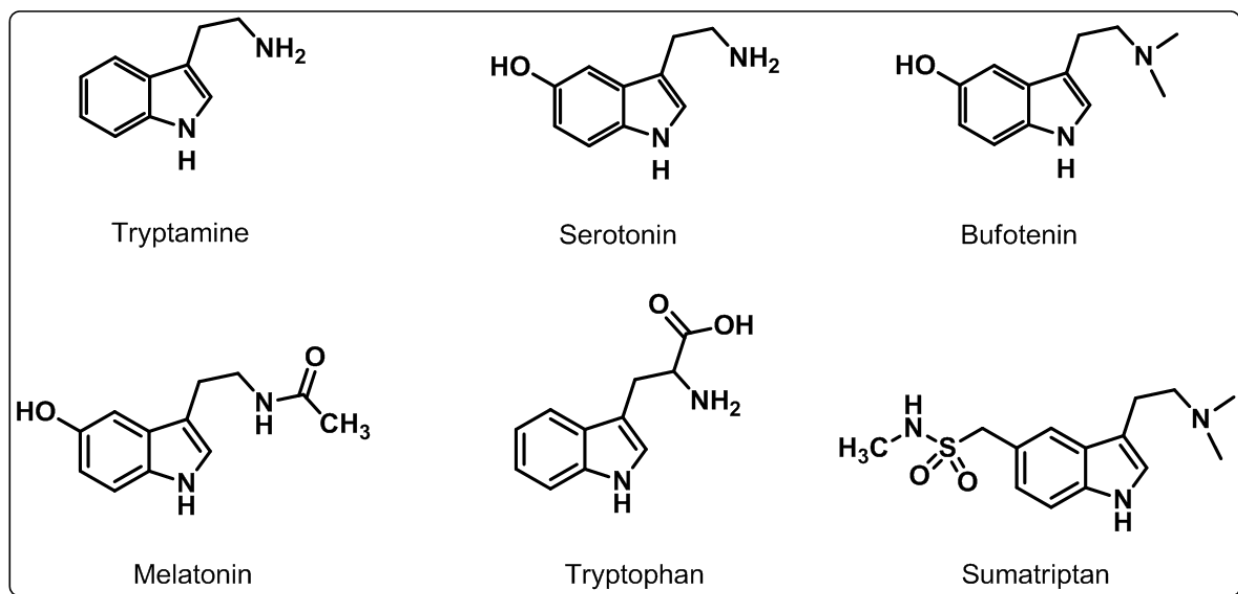


Figure 1. Representative examples of bioactive 3C-substituted indoles.

Results and discussion

Synthesis and characterization of nanocomposites

The nanocomposites of MoS₂-GCN were prepared by a facile ultrasonication route using appropriate precursors. In this work, MoS₂ amount in GCN nanosheets was varied to form MoS₂-GCN(1:1), MoS₂-GCN(1:2) and MoS₂-GCN(1:4) nanocomposites. To determine the structure of the as-prepared nanocomposites and bare catalysts, x-ray diffraction (XRD) measurements were performed and the results are presented in Figure 2 (a). It can be seen that GCN exhibits two distinct diffraction peaks at the 2θ values of 13.0° and 27.5°, which are assigned to (100) and (002) reflection planes, respectively. The strong diffraction peak at 27.5° corresponds to interlayer d-spacing of 0.336 nm of GCN and represents the stacking of the conjugated double bonds, while the weak diffraction peak at 13.0° corresponds to an interplanar separation of 0.672 nm.⁵⁵ These two diffraction peaks are in good agreement with reported literature (JCPDS 87-1526) for GCN.⁵⁵ The XRD pattern of MoS₂ has three discernible diffraction peaks at the 2θ values of 14.2°, 32.5°, and 57.0° which could be indexed to the (002), (100) and (110) reflection planes of crystalline MoS₂ as previously reported (JCPDS no. 37-1492).⁵⁶ The main diffraction at around 14.2° indicates the lamellar structure of layered MoS₂ nanosheets and corresponds to a d-spacing of 0.62 nm. It is noteworthy to mention here that the MoS₂-GCN (1:1) nanocomposite shows all diffraction peaks corresponding to both MoS₂ and GCN, confirming the successful synthesis of the nanocomposite.

FTIR spectra provide useful structural insights into bare catalysts and nanocomposites. From the results presented in Figure 2(b), it can be seen that bare GCN exhibits a series of peaks related to its polymeric structure. The broad absorption band in 3500-3000 cm⁻¹ originates from the stretching vibration of N-H bonds, associated with uncondensed amino groups, whereas a series of peaks in 1600-1200 cm⁻¹ could be assigned to the stretching vibrations of C-N heterocycles.⁵⁵ The above distinct mode of vibrations confirms the formation of C-N-C bonds in a graphitic material. Furthermore, the sharp peak at 806 cm⁻¹ could be assigned to the distinct breathing vibrations of the 1,3,5-triazine ring. As can be seen from the FTIR spectrum of bare MoS₂, the band at 467 cm⁻¹ could be assigned to the stretching vibration of the Mo-S bond.⁵⁷ The

FTIR spectrum of MoS₂-GCN(1:1) nanocomposite shows the presence of similar peaks as of bare GCN, verifying that the structure of GCN remains unchanged even after the nanocomposites formation with MoS₂.

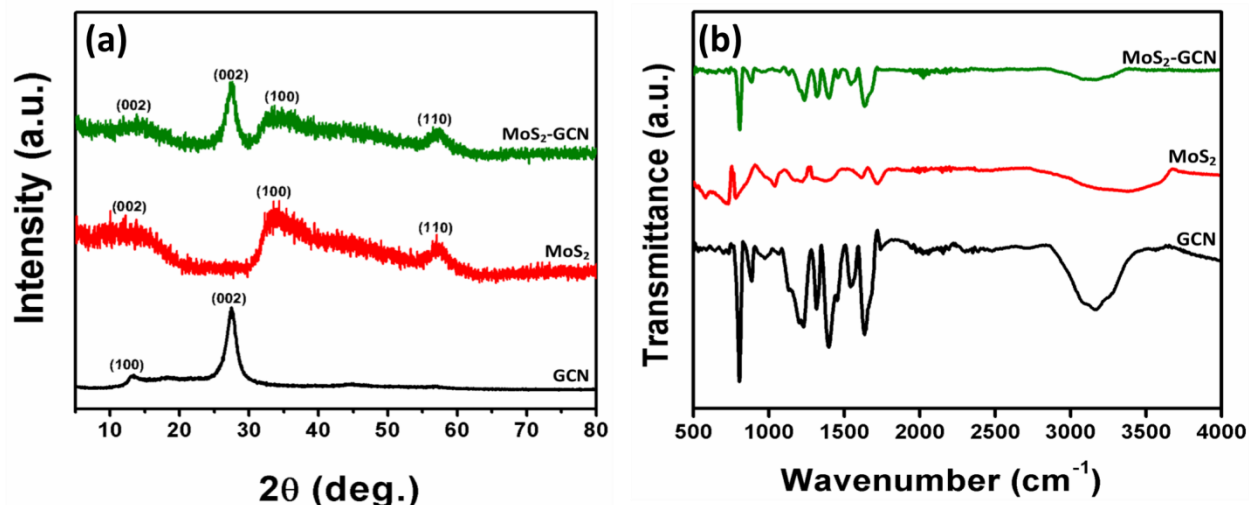


Figure 2.(a) XRD patterns of GCN, MoS₂and MoS₂-GCN(1:1) nanocomposite and (b) FTIR spectra of GCN, MoS₂and MoS₂-GCN(1:1) nanocomposite.

The morphology of as-prepared catalysts MoS₂, GCN and MoS₂-GCN (1:1) nanocomposite were analyzed by field emission scanning electron microscopy (FESEM) technique and are presented in Figure 3. It is clear from Figure 3(a) that, bare GCN exhibit wrinkled, sheet-like morphology with smooth surface. The SEM micrograph of MoS₂ also shows aggregated sheet-like morphology to form groove-like structure (Figure 3b). In the SEM images of MoS₂-GCN (1:1) nanocomposite, sheet-like layered structure of MoS₂ adhered on the surface of GCN nanosheets could be evidenced (Figure 2c). Hence, it is clear that MoS₂ is well dispersed onto GCN nanosheets to form the desired nanocomposite. Furthermore, the presence of all constituent elements (Mo, S, C, and N) in MoS₂-GCN (1:1) nanocomposite has been affirmed by energy dispersive x-ray (EDAX) technique as presented in Figure S1 (a).

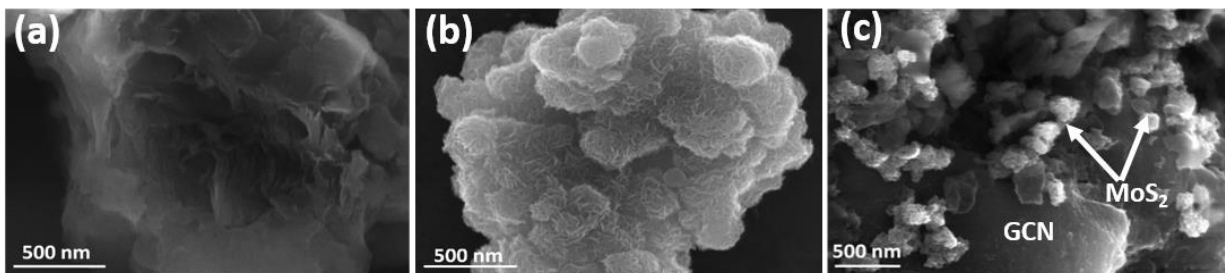


Figure 3. SEM images of (a) GCN, (b) MoS₂ and (c) MoS₂-GCN (1:1) nanocomposite.

Furthermore, transmission electron microscopy (TEM) analysis was used to further investigate the surface morphology of MoS₂, GCN and MoS₂-GCN (1:1) nanocomposite at nanometer scale and the obtained TEM images have been presented in Figure 3. Bare GCN shows thin sheet-like morphology of π -conjugated polymeric structure of C and N atoms (Figure 4a). It can be clearly seen in Figure 4(b) that MoS₂ shows lamellar structure. The TEM image of MoS₂-GCN (1:1) nanocomposite in Figure 4(c) reveals the presence of both components MoS₂ and GCN confirming the successful formation of the nanocomposite showing intimate contact between MoS₂ and GCN. All the constituent elements in representative MoS₂-GCN (1:1) nanocomposite were further confirmed by EDAX analysis presented in Figure S1 (b).

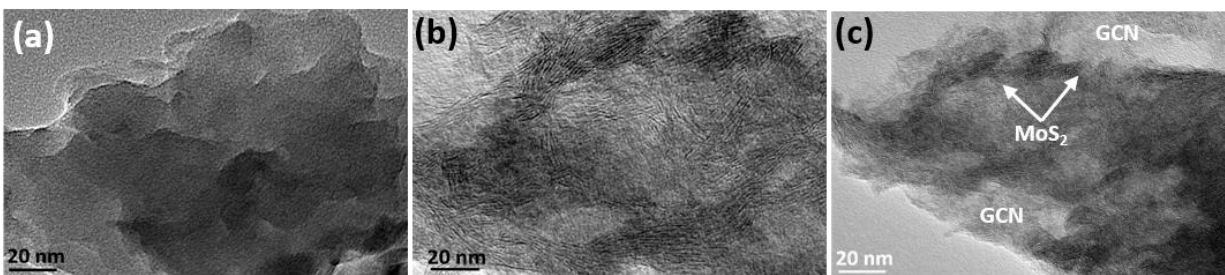


Figure 4. TEM images of (a) GCN, (b) MoS₂ and (c) MoS₂-GCN (1:1) nanocomposite.

The adsorption capacity of the catalysts is an important factor for understanding the catalytic reaction. In this regard, Brunauer–Emmett–Teller (BET) surface area measurements of bare GCN, MoS₂, and MoS₂-GCN (1:1) nanocomposite were performed by using nitrogen adsorption-desorption isotherms and are presented in Figure 5. The Figure 5(a, b, c) presents the isotherm curves of GCN, MoS₂ and MoS₂-GCN (1:1) nanocomposite together with corresponding multipoint BET plots (Figure 5 d, e, f), respectively. The adsorption–desorption isotherms of all three catalysts exhibit characteristic type IV curve with a hysteresis loop. The

MoS₂-GCN (1:1) nanocomposite was found to exhibit the largest surface area, 35.154 m²g⁻¹, while the surface area of the bare GCN was 20.099 m²g⁻¹ and that of MoS₂ was 21.982 m²g⁻¹. The increased specific surface area of MoS₂-GCN (1:1) nanocomposite resulted from the combination of 2D structures of GCN and MoS₂ nanosheets to form a hybrid material.

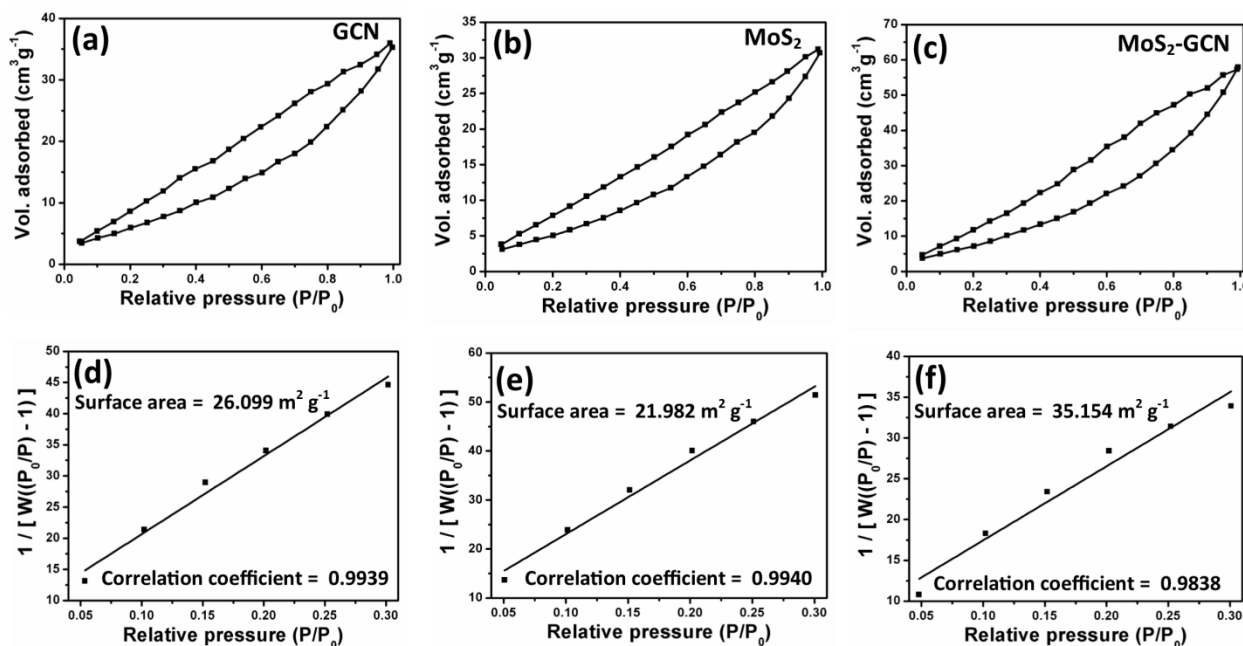


Figure 5. N₂ adsorption-desorption isotherms of (a) GCN, (b) MoS₂, (c) MoS₂-GCN (1:1) nanocomposite and multipoint BET plots of (d) GCN, (e) MoS₂, and (f) MoS₂-GCN (1:1) nanocomposite.

Thermogravimetric analysis (TGA) was performed to analyze the thermal stability of GCN, MoS₂ and MoS₂-GCN (1:1) nanocomposite (Figure 6) under the N₂ atmosphere from 25°C to 800°C. As it is evident from Figure 6, the decomposition of GCN starts after 500°C and about 98% degradation completes around 740°C, attributable to the burning of GCN into carbon and nitrogen. While, the slight decrease in weight of MoS₂ starts at 100°C, which indicates the loss of intercalated water molecules and again another weight loss of about 11% at 300°C attributed to the oxidation of MoS₂ to MoO₃. Similarly, for MoS₂-GCN nanocomposite loss of weight was observed after 500°C which resembles to weight loss due to GCN decomposition. Furthermore, this weight loss of about 52% in MoS₂-GCN nanocomposite also confirms the amount of MoS₂:GCN (1:1) in nanocomposite.

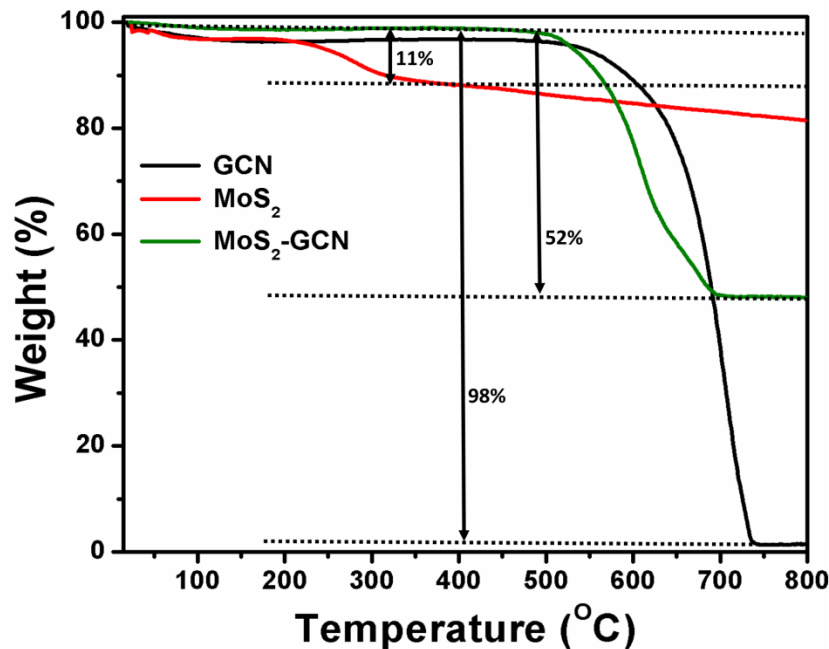


Figure 6. TGA profile of GCN, MoS₂ and MoS₂-GCN (1:1) nanocomposite.

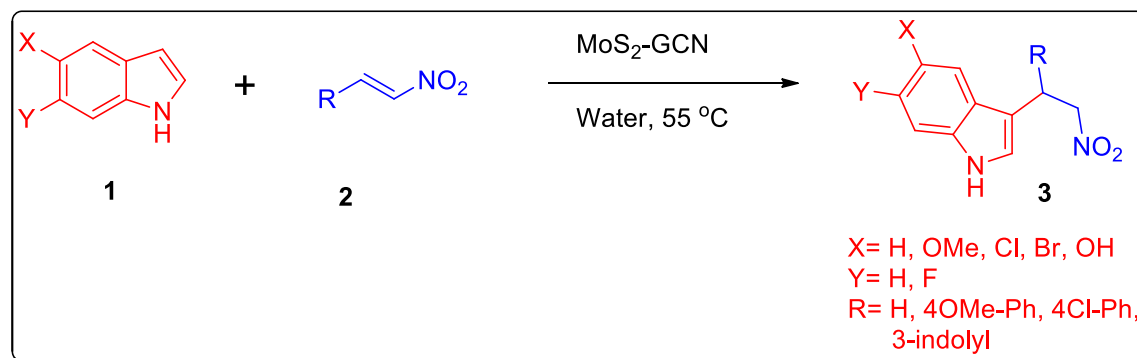
Hydrophilicity study has been carried out by contact angle measurement, in which water contact angle of GCN, MoS₂ and MoS₂-GCN nanocomposite were measured (Figure S2, refer supporting information). GCN showed a water contact angle of 51°, which shows very good hydrophilicity of the material. MoS₂ showed 86°, which reveals its tendency towards less hydrophilicity in comparison to GCN. Finally water contact angle of MoS₂-GCN (1:1) nanocomposite was measured, and it was found to be 69°, which is in intermediate range between more hydrophilic GCN and less hydrophilic MoS₂. We observed from our study that this intermediate range of hydrophilicity of the catalyst favors the reaction to undergo efficiently in aqueous medium.

Catalytic activity studies

The inherent catalytic potential of MoS₂-GCN nanocomposite has been investigated for the synthesis of 3C-functionalized indole derivatives by reaction of indoles with nitroalkenes and isatin. The catalytic activity of MoS₂-GCN nanocomposite was initially investigated on a model reaction of indole and beta-nitrostyrene to obtain a 3-(2-nitro-1-phenylethyl)indole using 10 wt % of the catalyst in water at 55°C (Scheme 1). Optimization studies have been

shown in Table 1, which shows that the nanocomposites with different ratios of MoS₂-GCN were prepared and evaluated for their catalytic potential. Reactions were performed with nanocomposite comprising 1:1, 1:2 and 1:4 ratios of MoS₂ and GCN, respectively. Initially reactions were performed at room temperature with the varying amount of catalyst but the yields were found to be very poor. When reactions were tried at higher temperatures, significant improvement in yields was observed. As it is evident from the optimization results (Table 1), that 10 wt % of MoS₂-GCN (1:1) nanocomposite was found to be the best catalyst, which resulted in 96% yield. When 20 wt% of MoS₂-GCN (1:1) nanocomposite was used in the reaction, not much difference in reactivity was observed. But when the reaction was tried with bare MoS₂, the formation of some unknown side products was observed which resulted in the decrease in yield of the reaction. Finally, reaction was performed with bare GCN, but no reactivity was observed after 12h also.

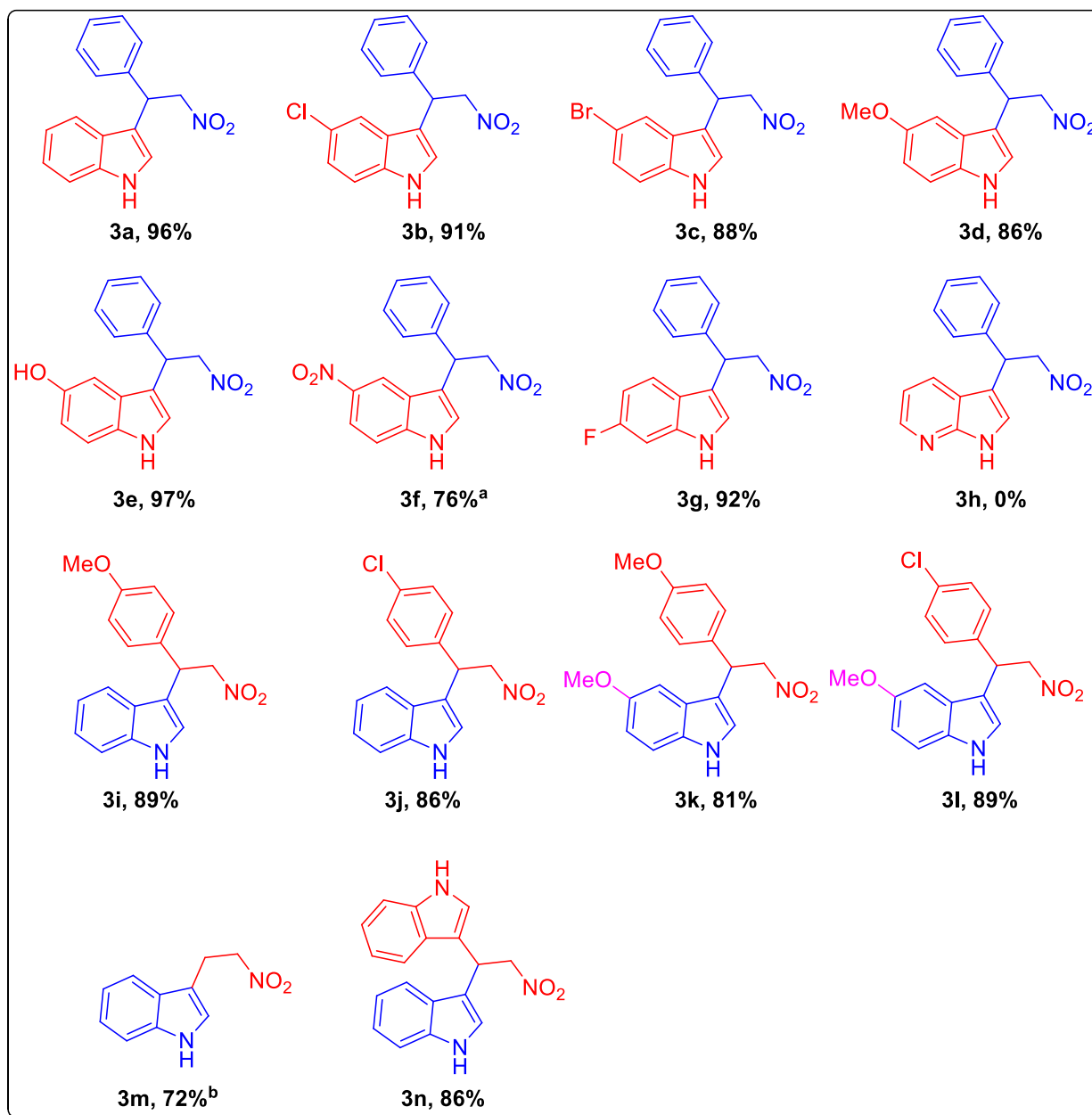
In order to extend the substrate scope and generality of MoS₂-GCN nanocatalytic system, various substituted indoles and nitroalkenes were tried (Table 2). Reactions were performed with indoles having fluoro, chloro, bromo, methoxy, nitro and hydroxyl functionalities, which demonstrated the good substrate scope with both electron withdrawing and electron donating groups present on indole rings. Since reaction was not successful at 55°C in case of 5-nitroindole, hence reaction was performed at 90°C to get the desired product. 7-azaindole being exceptional was found to be reluctant towards nitroalkenes, unlike other indoles. Similarly reactions were performed with varying electron withdrawing and electron donating groups at nitroalkene moiety, but it has no effect on reactivity of the catalyst. Moreover, the reaction was also performed with other Green solvents, such as ethyl acetate (EtOAc), ethanol (EtOH) and isopropyl alcohol (IPA) to see the change in reactivity with different other solvents. It was evidenced that the reactions in EtOH proceeded better than the reactions in EtOAc and IPA (Table 2, entry 17-20) under the similar reaction conditions.

Scheme 1. MoS₂- GCN catalyzed Green synthesis of 3C- functionalized indoles**Table 1.** Optimization of MoS₂-GCN catalyzed Michael type synthesis of 3-(2-nitro-1-phenylethyl)-1H-indole

Sl.No.	Catalyst	Catalyst wt%	Temp. (°C) and solvent	Time (h)	% Yield
1	MoS ₂ -GCN (1:1)	5	RT, H ₂ O	12	Trace
2	MoS ₂ -GCN (1:1)	5	RT, H ₂ O	24	15
3	MoS ₂ -GCN (1:1)	8	RT, H ₂ O	24	22
4	MoS ₂ -GCN (1:1)	10	RT, H ₂ O	24	32
5	MoS ₂ -GCN (1:1)	10	40, H ₂ O	12	45
6	MoS ₂ -GCN (1:1)	10	55, H ₂ O	12	96
7	MoS ₂ -GCN (1:1)	6	55, H ₂ O	12	95
8	MoS ₂ -GCN(1:1)	6	55, H ₂ O	24	81
9	MoS ₂ -GCN (1:1)	20	55, H ₂ O	12	91
10	MoS ₂ -GCN (1:2)	10	55, H ₂ O	12	53

11	MoS ₂ -GCN (1:2)	20	55, H ₂ O	12	67
12	MoS ₂ -GCN(1:4)	10	55, H ₂ O	12	20
13	MoS ₂	10	55, H ₂ O	12	69
14	MoS ₂	10	55, H ₂ O	24	51
15	GCN	10	55, H ₂ O	12	00
16	No catalyst	00	55, H ₂ O	12	00
17	MoS ₂ - GCN (1:1)	10	55, EtOAc	12	54
18	MoS ₂ - GCN (1:1)	10	55, IPA	12	63
19	MoS ₂ - GCN (1:1)	10	55, EtOH	12	72
20	MoS ₂ - GCN (1:1)	20	55, EtOH	12	78

Table 2. Substrate scope for the synthesis of 3C-functionalized indole derivatives of nitroalkenes



^a Reaction was performed at 90 °C temperature and ^b reaction was performed in ethanol instead of water.

Furthermore, to investigate the wide applicability of MoS₂-GCN, we performed reactions of indoles with isatin. A model reaction of indole and isatin was performed similar to the above

reaction. But in case of the reaction of indole with isatin, interesting results were obtained. When the reaction was performed at ambient temperature, the product formed was different from the product obtained by performing reaction at 55 °C (Scheme 2). When reaction of indole and isatin was carried out at room temperature, 3-hydroxy-3-(1H-indol-3-yl)indolin-2-one (Table 4, 6a) was observed as major product, but [3,3':3',3''-terindolin]-2'-one was found to be the major product when the same reaction was carried out at 55°C (Table 4, 5a). Optimization of reaction conditions have been presented in Table 3, and similar to the reaction with beta-nitrostyrene, the best catalytic system for reaction of indole with isatin was found to be 10 wt% of MoS₂-GCN (1:1). Wide substrate scope was observed by varying the substituent at indole and isatin (Table 4). Reactivity of isatin was found to be equally good with indoles having electron withdrawing or electron donating groups except for 5-nitroindole. Again, reaction with 5-nitroindole was performed at 90°C, while rest of all the reactions were carried out at 55°C (Table 4, 5a-5d & 5f-5i).

Scheme 2. Synthesis of 3C- functionalized indole derivatives of isatin

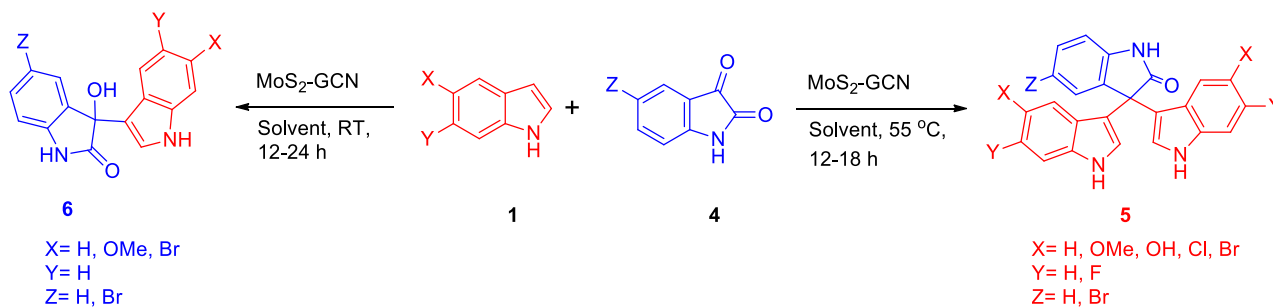
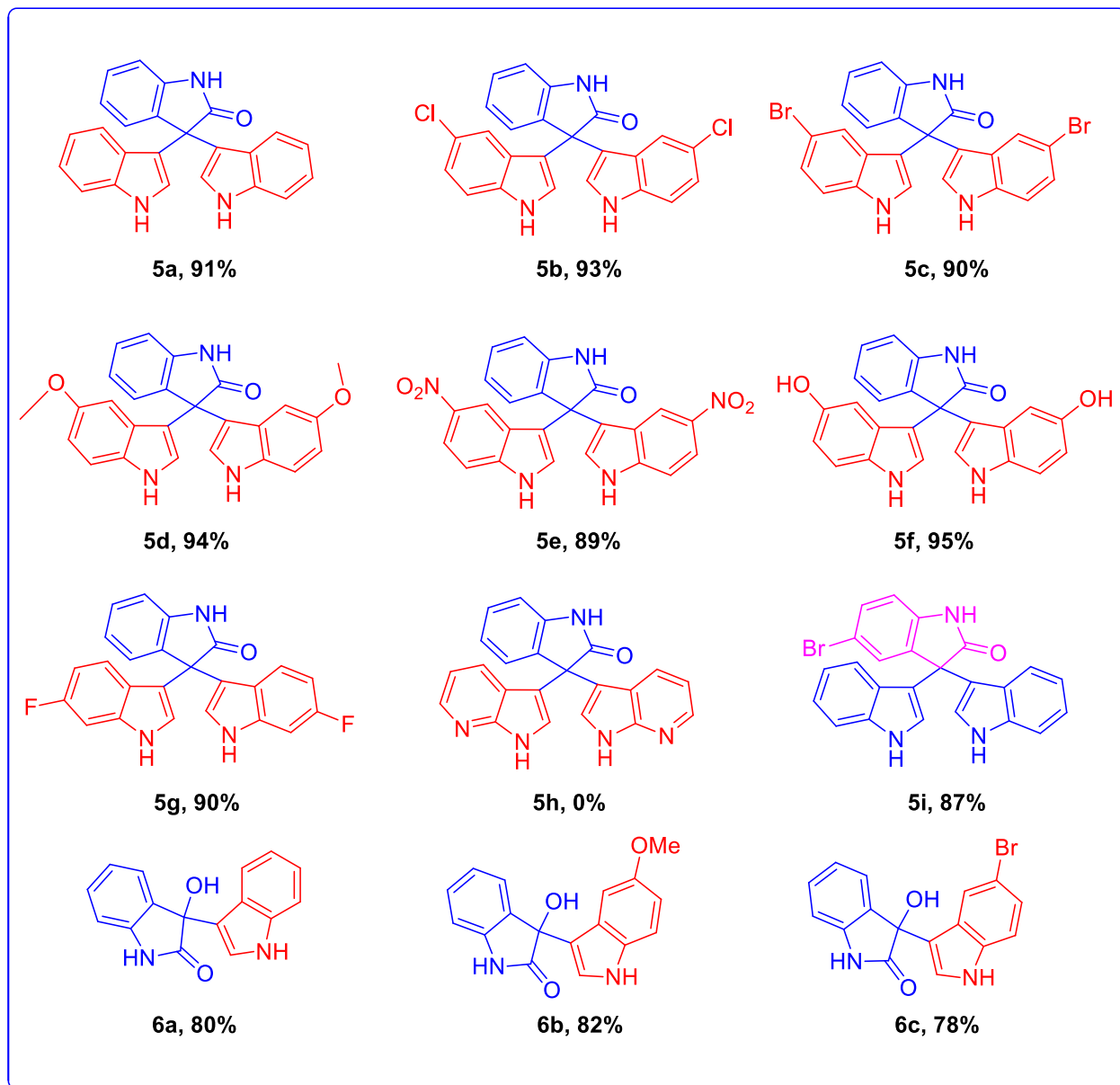
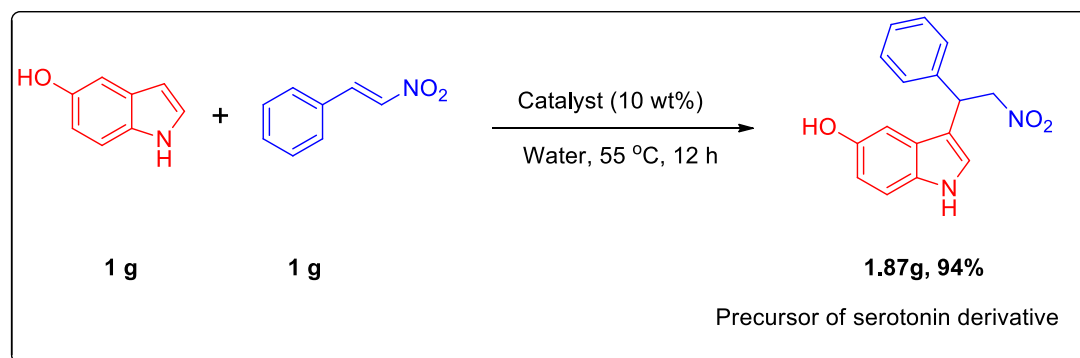


Table 3. Optimization of MoS₂-GCN catalyzed synthesis 3C- functionalized indole derivatives of isatin

Sl.No.	Catalyst	Catalyst	Temp.	Time (h)	% Yield

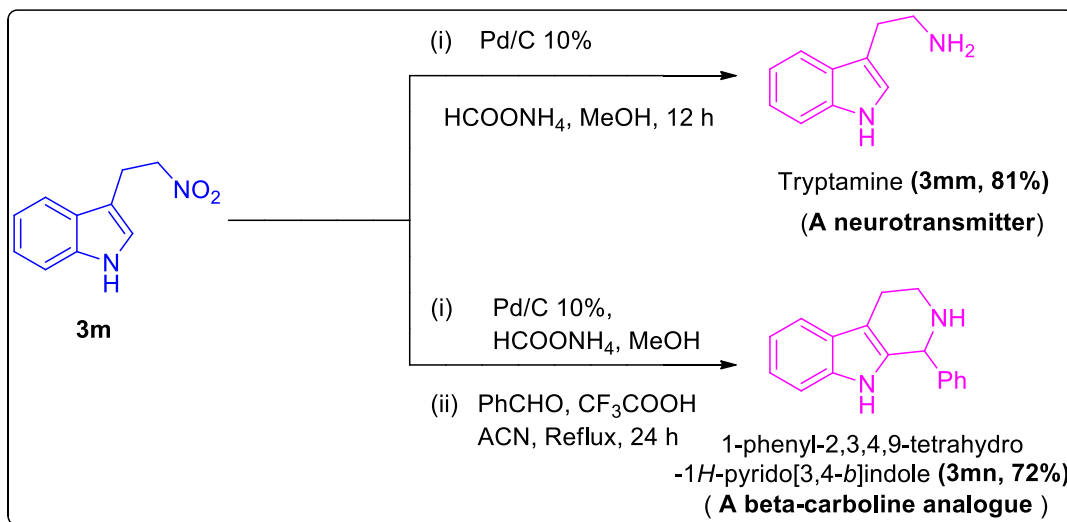
		wt%	(°C)		5a	6a
1	MoS ₂ -GCN (1:1)	5	RT	12	Trace	63
2	MoS ₂ -GCN (1:1)	8	RT	24	10	72
3	MoS ₂ - GCN(1:1)	5	55	12	38	54
4	MoS ₂ -GCN (1:1)	10	55	12	91	08
5	MoS ₂ -GCN (1:1)	10	40	12	59	37
6	MoS ₂ - GCN (1:1)	20	55	12	90	09
7	MoS ₂ -GCN (1:2)	10	55	12	20	45
8	MoS ₂ -GCN (1:2)	10	55	18	39	50
9	MoS ₂ -GCN (1:2)	10	55	24	63	36
10	MoS ₂ -GCN (1:4)	5	55	12	07	29
11	MoS ₂ -GCN (1:4)	10	55	24	12	36
12	MoS ₂	10	55	12	63	18
13	GCN	10	55	12	00	00
14	MoS ₂ - GCN (1:1)	10	RT	12	05	63
15	MoS ₂ - GCN (1:1)	10	RT	24	12	81
16	MoS ₂ - GCN (1:1)	20	RT	12	27	62
17	MoS ₂	10	RT	12	20	54

Table 4. Substrate scope for the synthesis of 3C-functionalized indole derivatives of isatin

Scheme 3. Gram-Scale Synthesis of 3-(2-nitro-1-phenylethyl)-1H-indol-5-ol (**3e**)

Pharmaceutical or other industrial benefits of the developed catalytic system could be demonstrated by performing a gram-scale reaction (Scheme 3) for the synthesis of **3e**, a precursor of substituted tryptamine (phenyl derivate of serotonin precursor). Starting from 1g of 5-hydroxyindole, and 1 g of beta-nitrostyrene, 1.87 g (94%) of product **3e** was obtained. This result reveals the potential of our catalyst for pharmaceutical industrial application, wherein reaction could be carried out at large-scale for the synthesis of substituted tryptamine precursor in mild reaction conditions using water as a solvent. For a standard sustainable and Green reaction, atom economy (AE)/ reaction mass efficiency (RME) should be high, and environmental factor(E-factor)along with process mass intensity(PMI) should be low⁴⁶. We have calculated Green chemistry matrices for our developed and optimized reaction, and found very high atom economy (A.E. = 100%), good reaction mass efficiency (R.M.E. = 95.9%) and small environmental factor (E-factor = 0.042) and low process mass intensity (P.M.E. = 1.042) (refer supporting information).

Scheme 4. Further transformation of **3m** to synthesize some bioactive scaffolds

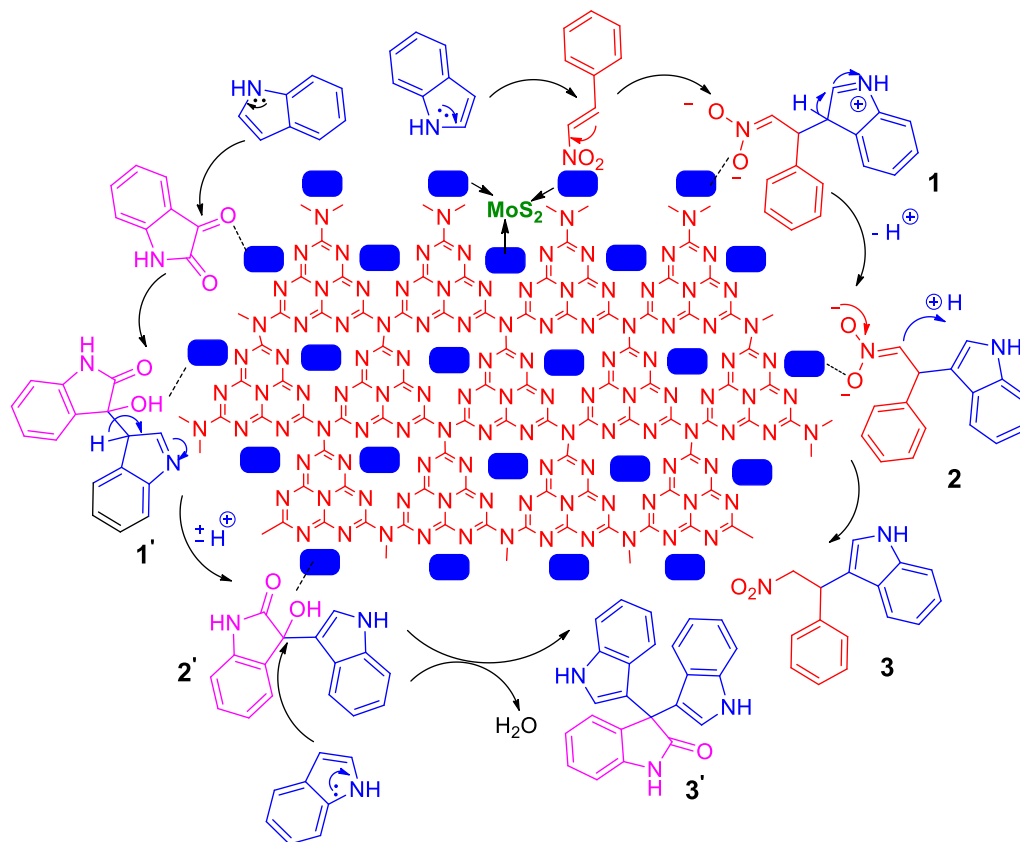


Furthermore, we also synthesized two bioactive molecules, tryptamine (**3mm**) and a beta-carboline analogue (**3mn**) to show the biological/ medicinal significance of the developed molecules. The structure of **3mn** has been reconfirmed by single crystal x-ray diffraction experiment (CCDC 1821503, Figure S3). Our developed protocol gives access to easy one or two-step synthesis of various substituted tryptamine (i.e. neurotransmitter such as, serotonin) and beta-carboline alkaloids, unlike several other multi-step synthesis methods.

Table 5. Comparison of catalytic activity of MoS₂- GCN with other metal/support based catalysts for synthesis of 3-substituted indoles

Entry	Product	Catalyst	Solvent	Time	Yield (%)	Ref
1	3a	Organopalladium(II) complexes	DCM	10 days	99	58
2	3a	NHC complexes of Ni(II) and Hg(II)	DCM	24h	85-86	59
3	3a	HY zeolite	Neat	1h	93	60
4	3a	Urea based MOF	ACN	18h	98	61
5	3a	Squaramide-based MOF	CHCl ₃	24h	99	62

6	3a	Gold(I)-mediated thiourea organocatalyst	DCM	18h	93	63
7	3a	Silica-supported sodium hydrogen sulfate	ACN	0.5h	84	64
8	3a	CeCl ₃ ·7H ₂ O-Nal supported on SiO ₂	ACN	8h	96	65
9	3a	Nano n-propylsulfonated γ -Fe ₂ O ₃	Neat	1h	85	66
10	3a	Cationic NCN Pincer Platinum(II) Aquo Complex	Toluene	36h	81	67
11	3a	Nanocrystalline titanium(IV) Oxide	DCM	4h	79	68
12	3a	MoS ₂ -GCN	Water	12h	96	This work
13	5a	Bismuth(III) triflate	ACN	3h	92	69
14	5a	Silica sulfuric acid	DCM	2 h	92	70
15	5a	MoS ₂ -GCN	Water	12 h	91	This work

Scheme 5. Mechanism of catalytic activity of MoS₂-GCN nanocomposite

In general, MoS₂ is a Lewis acid catalyst and GCN is a base catalyst. Although bare MoS₂ shows some catalytic activity, the nanocomposite comprising of MoS₂ and GCN shows excellent activity, which could be attributed to the synergistic effects due to the formation of Lewis acid-base non-bonding adducts. The mechanism of the proposed catalytic cycle is shown in Scheme 5. As depicted in the scheme, MoS₂ makes the nitrostyrene more electron-deficient and prone to attack by a nucleophile. Furthermore, GCN being a base facilitates the proton transfer during the reaction. The catalytic cycle shows that, at the surface of catalyst the electron deficient alkene (beta nitrostyrene) due to its electrophilic nature gets attacked by 3-position of indole. Then the reaction proceeds in a fashion similar to Michael addition and forms an intermediate 2, which after exchanging the proton forms the product 3. Similarly, isatin also becomes more electrophilic at the catalyst surface and easily gets nucleophilic attack by indole molecule to

form a hydroxyl intermediate 2'. The hydroxyl intermediate 2' then again gets attacked by another indole molecule to form the final product 3' after removal of a water molecule. The hydroxyl intermediate can be isolated if the experiment is performed in controlled conditions (i.e. either by performing reaction at RT or by using equal moles of indole and isatin). Finally, the recyclability studies were performed for the MoS₂-GCN (1:1) nanocomposite catalyst for the synthesis of 3-substituted indole 3a under the optimized reaction conditions as per Table 1. There was no significant loss in activity of the catalyst even after 6 cycles (refer Figure 7). The small decrease in activity between the different cycles could be attributed to the loss of small amount of catalyst during recovery process.

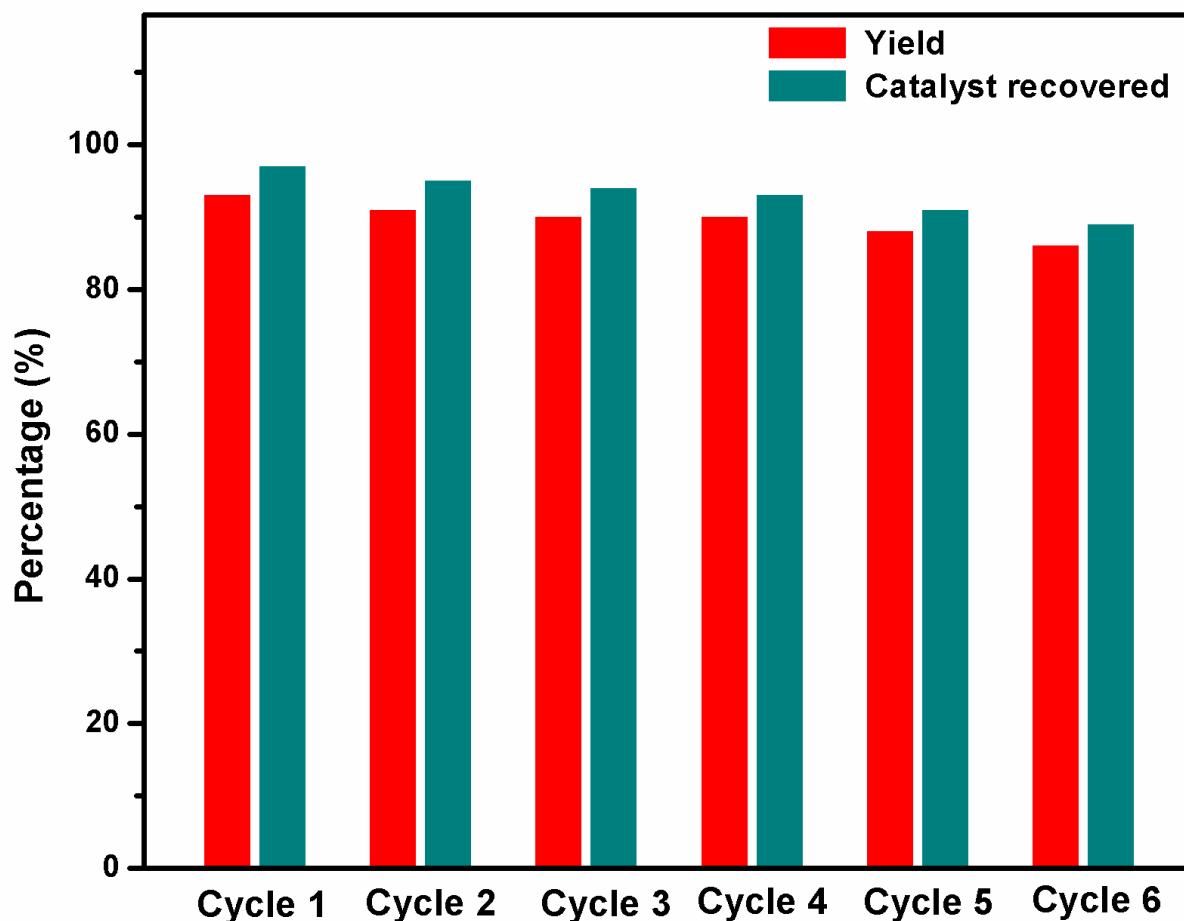


Figure 7. Recyclability study of MoS₂-GCN (1:1) nanocomposite catalyst for the synthesis of 3C-functionalized indole 3a.

Conclusion

In summary, it has been demonstrated that MoS₂-GCN nanocomposites act as highly efficient and recyclable heterogeneous multifunctional catalyst for the synthesis of various 3-C functionalized indoles. The MoS₂-GCN catalytic system has several advantages such as high catalytic performance, good yields in moderate reaction times, applicability to a wide range of indole-based organic reactions and use of water as a Green solvent. The MoS₂-GCN catalyst can be easily recovered from reaction mixtures and recycled multiple times without significant loss in activity. In addition, the high atom economy (99%) and lower E-factor (0.042) makes this strategy a sustainable approach for the synthesis of several bioactive indole derivatives.

Experimental Section

Instrumentation

X-ray diffraction (XRD) measurements were performed on Rigaku Smart Lab 9 kW rotating anode X-ray diffractometer with Ni-filtered Cu K α irradiation ($\lambda = 0.1542$ nm) at 45 kV and 100 mA in 2θ ranging from 5° to 80° with a scan rate of 2° per minute with stepping size of 0.02°. Morphology of the materials was examined by using a field emission scanning electron microscope (FESEM), FEI Nova Nano SEM-450, and a transmission electron microscope (TEM), FEI Tecnai G2 20 S-twin microscope operating at 200 kV. Energy dispersive X-ray spectra (EDAX) were acquired using the same SEM and TEM instruments. X-ray photoelectron spectroscopic (XPS) measurements were performed on a PREVEC photoemission spectrometer having an Al-K α (1486.6 eV) dual anode as a source operating a 12 kV anode and 23 mA filament current. The XPS data were collected with a pass energy of 50 eV at 6.1×10^{-10} m bar vacuum using a Scienta R3000 electron energy analyzer. The data obtained from the instrument were processed and deconvoluted using CASA software. Thermogravimetric analysis (TGA) was carried out by using a PerkinElmer Pyris 1 instrument, wherein the samples were heated from room temperature to 800 °C at a heating rate of 10 °C min⁻¹ under the air with a flow rate of 20 mL min⁻¹. Contact angle measurements were performed using the Phoenix 300 contact angle instrument. Melting points were determined using an open capillary method. NMR spectra were recorded on a

JEOL-USA (JNMECX500) spectrometer in CDCl_3 and DMSO-d_6 taking TMS (tetramethylsilane) as an internal standard. The $^1\text{H-NMR}$ and $^{13}\text{C-NMR}$ chemical shifts were reported in ppm relative to 7.26, 2.50 ppm, and 77.0 and 39.5 ppm, for CDCl_3 and DMSO-d_6 . $^1\text{H-NMR}$ spectra were recorded in 500 MHz frequency, and $^{13}\text{C-NMR}$ spectra were recorded at 125 MHz frequency. FT-IR spectra were acquired on a PerkinElmer Spectrum 2 spectrometer. Mass spectra were recorded on an advance Bruker Daltonics (impact HD) UHR-QqTOF (ultra-high resolution Qqtime-of-flight) mass spectrometer. Synthesis of catalyst and all the reactions were carried out in deionized water (18.2 $\text{M}\Omega\text{ cm}$), which was obtained from a double stage water purifier (ELGA PURELAB Option-R7).

Chemicals

All of the necessary chemicals were procured from Sigma Aldrich, Fluka, Alfa Aesar, Merck, and TCI suppliers based in India. For MoS_2 nanosheets synthesis, sodium molybdate dihydrate ($\text{Na}_2\text{MoO}_4 \cdot 2\text{H}_2\text{O}$) was purchased from by Merck, India and L-Cysteine (98%) was supplied by Alfa Aesar, India. Hexane and ethyl acetate for column chromatography was supplied by Fischer Scientific and AVRA chemicals, respectively.

Synthesis of MoS_2 nanosheets

MoS_2 nanosheets were prepared by referring a reported procedure.⁷¹ In short, 250 mg of sodium molybdate dihydrate, 400 mg of L-cysteine and 40 mL of de-ionised water were mixed in a 100 mL beaker and kept on stirring for 1h. Followed by stirring, the reaction mixture was then transferred into a Teflon-lined autoclave and temperature was maintained at 180°C for 24h. The obtained material was recovered by centrifugation at 7000 rpm followed by repeated washing with water for 3-4 times. Finally, the material was dried at $70\text{-}80^\circ\text{C}$ for 12h to obtain pure MoS_2 nanosheets.

Synthesis of GCN nanosheets

Graphitic carbon nitride (GCN) nanosheets were prepared by a reported literature method. In brief, 5 g of dicyandiamide was taken in a crucible and heated at 550°C (at a rate of 5°C per

minute) in a muffle furnace for 3h. After this step, the material was crushed to powder in a mortar-pestle and re-calcinated again at 550°C for 3h to obtain the final product.

Synthesis of MoS₂-GCN nanocomposite

MoS₂-GCN nanocomposite was synthesized by ultrasonic dispersion method⁷² described here. Firstly, 200 mg of the synthesized GCN powder was dissolved in 20 mL of ethanol and varying amounts (50,100,200 mg) of MoS₂ was added to make nanocomposites in different ratios (1:4, 1:2 and 1:1). The mixture was stirred for 3h followed by ultrasonic dispersion for another 3h. Finally, obtained composites were centrifuged and washed with water and ethanol (3 times) and dried at 70°C for 12h. Three different nanocomposites of MoS₂-GCN (1:1, 1:2, and 1:4) were fabricated varying MoS₂ content.

General procedure for synthesis of 3C-functionalized indole derivatives of nitroalkenes (3a - 3l)

In a 10 mL round bottomed flask, a mixture of indole (1 mmol), nitroalkene (1mmol), MoS₂-GCNcatalyst (10 wt %), and water (2 mL) were placed and stirred at 55°C temperature. Progress of the reaction was time-to-time monitored by TLC. After completion of the reaction, water was decanted from reaction and ethanol was added to the reaction mixture accompanied by centrifugation of reaction mixture to separate the nanocomposite catalyst. The organic layer was dried over sodium sulfate, and the solvent was removed using rotary evaporator under reduced pressure. The obtained crude product was purified by column chromatography. All the compounds were characterized by melting point, ¹H & ¹³C NMR spectral data.

General procedure for synthesis of 3C-functionalized indoles derivatives of isatin (5a- 5i)

In a 10 mL round-bottomed flask, a mixture of indole (1 mmol), isatin (0.5 mmol), MoS₂-GCN catalyst (10 wt %), and water (2 mL) were placed and stirred at 55°C temperature (with exception to the reaction of nitroindole and isatin, which was proceeded at 90°C). Progress of the reaction was monitored by TLC. After completion of the reaction, water was decanted from reaction and ethanol was added to the reaction mixture accompanied by centrifugation of

reaction mixture to separate the nanocomposite catalyst. The organic layer was dried over sodium sulfate, and the solvent was removed at rotary evaporator under reduced pressure. The obtained crude product was purified by column chromatography. All the compounds were characterized by melting point, ^1H & ^{13}C NMR spectral data.

Procedure for synthesis of 2-(1H-indol-3-yl)ethanamine (3mm) from 3-(2-nitroethyl)-1H-indole (3m)⁷³

To a stirring solution of compound **3m** (0.5 mmol) in methanol (2 mL) were added Pd/C 10% and HCOONH_4 (2.5 mmol). The reaction mixture was stirred at ambient temperature for 12 h. After completion of the reaction, mixture was filtered on a celite pad, and the pad was washed three times with methanol and the solvent was evaporated under reduced pressure. The solid residue was dissolved in EtOAc, washed with saturated Na_2CO_3 , brine, and the aqueous phase was extracted twice with EtOAc. The organic phase was dried over Na_2SO_4 and evaporated to afford compound **3mm** as a white-orange solid in 81% yield.

Procedure for the synthesis of 1-phenyl-2,3,4,9-tetrahydro-1H-pyrido[3,4-b]indole (3mn) from 3-(2-nitroethyl)-1H-indole (3m)⁷³

It is a two-step synthetic procedure in which the first step of the synthesis is the same as described above (i.e. 3m to 3mm). In the second step, to a stirred solution of crude **3mm** (0.5 mmol) in dry acetonitrile (9 mL), were sequentially added CF_3COOH (1.0 mmol) and benzaldehyde (0.55 mmol). The resulting solution was kept on stirring at 80 °C for 24h. After completion of the reaction, the mixture was cooled to ambient temperature and was poured into sat. NaHCO_3 and then extracted thrice with dichloromethane. The organic phase was dried over Na_2CO_3 and concentrated. The product was then isolated by chromatography on silica gel (EtOAc/Hexane (70:30) mixture) in 72% yield as a yellowish orange solid **3mn**.

Compound characterization

3-(2-nitro-1-phenylethyl)-1H-indole⁷⁴⁻⁷⁶: 92%, (R_f = 0.45, 15:85 EtOAc/Hex), ^1H NMR (CDCl_3 , 500 MHz) δ 8.05 (brs, 1H), 7.43 (d, 1H, J = 8.2 Hz), 7.33-7.28 (m, 5H), 7.26-7.22 (m, 1H), 7.18 (t, 1H, J

= 6.9 Hz), 7.06 (t, 1H, J = 6.9 Hz), 6.99 (d, 1H, J = 2.7Hz), 5.17 (t, 1H, J = 7.5Hz), 5.06-5.02 (m, 1H), 4.94-4.90 (m, 1H); ^{13}C NMR (CDCl_3 , 125 MHz) δ 139.1, 136.4, 128.9, 127.7, 127.5, 126.0, 122.6, 121.6, 119.9, 118.8, 114.3, 111.3, 79.5, 41.5.

5-chloro-3-(2-nitro-1-phenylethyl)-1H-indole⁷⁶:91%, (R_f = 0.5, 15:85 EtOAc/Hex), ^1H NMR (CDCl_3 , 500 MHz) δ 8.15 (brs, 1H), 7.37 (s, 1H), 7.33-7.22 (m, 6H), 7.12 (dd, 1H, J = 1.4 & 8.25 Hz), 7.05 (s, 1H), 5.11 (t, 1H, J = 7.6 Hz), 5.02-4.98 (m, 1H), 4.92-4.88 (m, 1H); ^{13}C NMR (CDCl_3 , 125 MHz) δ 138.7, 134.7, 129.0, 127.7, 127.6, 127.1, 125.6, 123.0, 122.8, 118.3, 114.0, 112.4, 79.3, 41.3.

5-bromo-3-(2-nitro-1-phenylethyl)-1H-indole⁷⁵:88%, (R_f = 0.5, 12:88 EtOAc/Hex), ^1H NMR (CDCl_3 , 500 MHz) δ 8.17 (brs, 1H), 7.53 (d, 1H, J = 1.3 Hz), 7.32-7.22 (m, 6H), 7.16 (d, 1H, J = 8.2 Hz), 7.00 (d, 1H, J = 2.7 Hz), 5.09 (t, 1H, J = 7.5 Hz), 5.00-4.96 (m, 1H), 4.91-4.86 (m, 1H); ^{13}C NMR (CDCl_3 , 125 MHz) δ 138.6, 135.0, 129.0, 127.8, 127.7, 127.6, 125.5, 122.7, 121.3, 113.8, 113.1, 112.8, 41.2.

5-methoxy-3-(2-nitro-1-phenylethyl)-1H-indole⁷⁶: 86%, (R_f = 0.40, 20:80 EtOAc/Hex), ^1H NMR (CDCl_3 , 500MHz) δ 8.01 (brs, 1H), 7.33-7.29 (m, 4H), 7.25-7.19 (m, 2H), 6.95 (s, 1H), 6.85-6.83 (m, 2H), 5.12 (t, 1H, J = 7.5 Hz), 5.04-5.00 (m, 1H), 4.93-4.89 (m, 1H), 3.76 (s, 3H); ^{13}C NMR (CDCl_3 , 125 MHz) δ 154.1, 139.1, 131.5, 128.9, 127.7, 127.5, 126.5, 122.2, 113.9, 112.6, 112.1, 100.7, 79.4, 55.8, 41.4.

3-(2-nitro-1-phenylethyl)-1H-indol-5-ol⁷⁷:97%, (R_f = 0.50, 40:60 EtOAc/Hex), ^1H NMR (CDCl_3 , 500 MHz) δ 8.10 (brs, 1H), 7.22-7.14 (m, 5H), 7.04 (d, 1H, J = 8.2 Hz), 6.83 (d, 1H, J = 2.05 Hz), 6.79 (d, 1H, J = 2.05 Hz), 6.70 (dd, 1H, J = 2.75 Hz & 6.1 Hz), 5.87 (s, 1H), 4.96 (t, 1H, J = 8.2 Hz), 4.88-4.84 (m, 1H), 4.79-4.75 (m, 1H); ^{13}C NMR (CDCl_3 , 125 MHz) δ 149.4, 139.0, 131.5, 128.7, 127.6, 127.4, 126.6, 122.6, 113.3, 112.4, 112.1, 103.3, 79.2, 41.4.

6-fluoro-3-(2-nitro-1-phenylethyl)-1H-indole⁶⁰:92%, (R_f = 0.40, 20:80 EtOAc/Hex), ^1H NMR (CDCl_3 , 500 MHz) δ 8.15 (brs, 1H), 7.29-7.19 (m, 6H), 6.94-6.92 (m, 2H), 6.79-6.75 (m, 1H), 5.10 (t, 1H, J = 8.2 Hz), 4.99-4.95 (m, 1H), 4.88-4.84 (m, 1H); ^{13}C NMR (CDCl_3 , 125 MHz) δ 160.9, 159.0, 138.9, 136.4, 136.3, 128.9, 128.7, 127.6, 127.6, 127.4, 122.6, 121.7, 119.6, 119.5, 114.1, 108.6, 108.4, 97.7, 97.5, 79.4, 41.3.

3-(1-(4-methoxyphenyl)-2-nitroethyl)-1H-indole⁷⁵: 81%, ($R_f = 0.40$, 25:75 EtOAc/Hex), ¹H NMR (CDCl₃, 500 MHz) δ 8.12 (brs, 1H), 7.43 (d, 1H, $J = 7.5$ Hz), 7.35 (d, 1H, $J = 8.2$ Hz), 7.25-7.17 (m, 3H), 7.08-7.01 (m, 2H), 6.84 (d, 2H, $J = 8.9$ Hz), 5.13 (t, 1H, $J = 7.5$ Hz), 5.06-5.02 (m, 1H), 4.91-4.87 (m, 1H); ¹³C NMR (CDCl₃, 125 MHz) δ 158.8, 136.5, 131.1, 128.8, 126.0, 122.6, 121.4, 119.9, 118.9, 114.7, 114.2, 111.3, 79.7, 55.2, 40.8.

3-(1-(4-chlorophenyl)-2-nitroethyl)-1H-indole⁷⁵: 86%, ($R_f = 0.5$, 20:80 EtOAc/Hex), ¹H NMR (CDCl₃, 500 MHz) δ 8.12 (brs, 1H), 7.38 (d, 1H, $J = 8.2$ Hz), 7.33 (d, 1H, $J = 8.2$ Hz), 7.27-7.18 (m, 5H), 7.07 (t, 1H, $J = 7.5$ Hz), 6.96 (s, 1H), 5.14 (t, 1H, $J = 7.5$ Hz), 5.04-5.00 (m, 1H), 4.89-4.85 (m, 1H); ¹³C NMR (CDCl₃, 125 MHz) δ 137.6, 136.4, 133.3, 129.1, 129.0, 125.8, 122.8, 121.5, 120.0, 118.7, 113.8, 111.4, 79.2, 40.0.

3-(1-(4-chlorophenyl)-2-nitroethyl)-5-methoxy-1H-indole⁶⁷: 89%, ($R_f = 0.40$, 25:75 EtOAc/Hex), ¹H NMR (CDCl₃, 500 MHz) δ 8.13 (brs, 1H), 7.27-7.19 (m, 6H), 6.93 (d, 1H, $J = 2.0$ Hz), 6.84 (dd, 1H, $J = 2.7$ Hz & 6.2 Hz), 6.78 (d, 1H, $J = 2.0$ Hz), 5.08 (t, 1H, $J = 8.2$ Hz), 5.01-4.97 (m, 1H), 4.87-4.83 (m, 1H), 3.76 (s, 3H); ¹³C NMR (CDCl₃, 125 MHz) δ 154.1, 137.6, 133.3, 131.5, 129.1, 129.0, 126.3, 122.2, 113.3, 112.7, 112.2, 100.6, 79.1, 55.8, 40.8.

5-methoxy-3-(1-(4-methoxyphenyl)-2-nitroethyl)-1H-indole⁷⁸: 81%, ($R_f = 0.40$, 40:60 EtOAc/Hex), ¹H NMR (CDCl₃, 500 MHz) δ 7.99 (brs, 1H), 7.25-7.23 (m, 4H), 6.99 (d, 1H, $J = 2.7$ Hz), 6.85-6.82 (m, 4H), 5.08 (t, 1H, $J = 15.8$ Hz), 5.04-5.00 (m, 1H), 4.90-4.86 (m, 1H), 3.77 (s, 6H); ¹³C NMR (CDCl₃, 125 MHz) δ 158.8, 154.1, 131.5, 131.1, 128.8, 126.5, 122.1, 114.4, 114.2, 112.7, 112.0, 100.8, 79.7, 55.8, 55.2, 40.8.

1H,1''H-[3,3':3',3''-terindol]-2'(1'H)-one⁷⁹: 91%, ($R_f = 0.40$, 40:60 EtOAc/Hex), ¹H NMR (DMSO-d₆, 500 MHz) δ 10.96 (s, 2H), 10.61 (s, 1H), 7.35 (d, 2H, $J = 8.2$ Hz), 7.24-7.21 (m, 4H), 7.03-6.98 (m, 3H), 6.92 (t, 1H, $J = 7.5$ Hz), 6.86 (d, 2H, $J = 2.7$ Hz), 6.80 (t, 2H, $J = 7.5$ Hz); ¹³C NMR (DMSO-d₆, 125 MHz) δ 178.7, 141.3, 136.9, 134.6, 127.8, 125.7, 124.9, 124.3, 121.4, 120.9, 120.8, 118.2, 114.3, 111.6, 109.6, 52.6.

5,5''-dichloro-1H,1''H-[3,3':3',3''-terbenzo[b]pyrrol]-2'(1'H)-one⁸⁰: 93%, ($R_f = 0.40$, 30:70 EtOAc/Hex), ¹H NMR (DMSO-d₆, 500 MHz) δ 11.22 (s, 2H), 10.74 (s, 1H), 7.39 (d, 2H, $J = 8.9$ Hz), 7.26 (dt, 1H, $J = 1.3$ Hz & 6.2 Hz), 7.19-7.17 (m, 3H), 7.05-6.9 (m, 4H), 6.93 (d, 2H, $J = 2.7$ Hz); ¹³C

NMR (DMSO- d_6 , 125 MHz) δ 178.4, 141.2, 135.4, 128.3, 126.6, 126.1, 124.9, 122.9, 121.8, 121.1, 119.6, 113.9, 113.4, 109.8, 52.1.

5,5''-dibromo-1H,1''H-[3,3':3',3''-terbenzo[b]pyrrol]-2'(1'H)-one⁸¹: 90%, (R_f = 0.50, 30:70 EtOAc/Hex), ¹H NMR (DMSO- d_6 , 500 MHz) δ 11.22 (s, 2H), 10.74 (s, 1H), 7.36-7.34 (m, 4H), 7.27 (t, 1H, J = 7.5 Hz), 7.17-7.14 (m, 3H), 7.02-6.97 (m, 2H), 6.90 (d, 2H, J = 2.7 Hz); ¹³C NMR (DMSO- d_6 , 125 MHz) δ 178.4, 141.2, 135.7, 133.6, 128.3, 127.2, 126.0, 124.9, 123.6, 122.6, 121.8, 113.8, 113.8, 111.0, 109.8, 52.1, 40.0.

5,5''-dihydroxy-1H,1''H-[3,3':3',3''-terbenzo[b]pyrrol]-2'(1'H)-one: 95%, (R_f = 0.50, 75:25 EtOAc/Hex), ¹H NMR (DMSO- d_6 , 500 MHz) δ 10.62 (s, 2H), 10.50 (s, 1H), 8.47 (s, 2H), 7.22-7.17 (m, 2H), 7.12 (d, 2H, J = 8.9 Hz), 6.96-6.90 (m, 2H), 6.69 (d, 2H, J = 2.7 Hz), 6.63 (d, 2H, J = 2.0 Hz), 6.53 (dd, 2H, J = 11 Hz & 6.8 Hz); ¹³C NMR (DMSO- d_6 , 125 MHz) δ 178.8, 149.7, 141.3, 134.7, 131.5, 127.6, 126.5, 124.7, 121.2, 113.2, 111.7, 111.3, 109.5, 105.1, 52.5.

5,5''-dinitro-1H,1''H-[3,3':3',3''-terbenzo[b]pyrrol]-2'(1'H)-one⁷⁹: 89%, (R_f = 0.40, 50:50 EtOAc/Hex), ¹H NMR (DMSO- d_6 , 500 MHz) δ 11.82 (s, 2H), 10.98 (s, 1H), 8.23 (d, 2H, J = 2.0 Hz), 7.95 (dd, 2H, J = 2.7 Hz & 6.8 Hz), 7.57 (d, 2H, J = 8.9 Hz), 7.31 (t, 1H, J = 7.5 Hz), 7.24-7.21 (m, 3H), 7.07 (d, 1H, J = 7.5 Hz), 7.01 (t, 1H, J = 7.5 Hz); ¹³C NMR (DMSO- d_6 , 125 MHz) δ 178.0, 141.2, 140.2, 132.9, 128.7, 128.3, 124.9, 124.6, 122.2, 117.5, 116.7, 112.5, 110.2, 52.1.

6,6''-difluoro-1H,1''H-[3,3':3',3''-terbenzo[b]pyrrol]-2'(1'H)-one: 90%, (R_f = 0.40, 40:60 EtOAc/Hex), ¹H NMR (DMSO- d_6 , 500 MHz) δ 11.05 (s, 2H), 10.65 (s, 1H), 7.21-6.69 (m, 12H); ¹³C NMR (DMSO- d_6 , 125 MHz) δ 174.5, 159.6, 157.7, 141.3, 136.8, 136.8, 134.1, 128.0, 124.8, 122.5, 121.7, 121.6, 114.4, 109.7, 107.0, 106.8, 97.6, 97.4, 52.3.

5'-bromo-1H,1''H-[3,3':3',3''-terbenzo[b]pyrrol]-2'(1'H)-one⁸²: 87%, (R_f = 0.40, 40:60 EtOAc/Hex), ¹H NMR (DMSO- d_6 , 500 MHz) δ 11.04 (s, 2H), 10.64 (s, 1H), 7.25-7.16 (m, 4H), 7.12 (d, 2H, J = 2.0 Hz), 6.96 (dd, 2H, J = 7.5 Hz & 9.6 Hz), 6.84 (d, 2H, J = 2.0 Hz), 6.70-6.66 (m, 2H); ¹³C NMR (DMSO- d_6 , 125 MHz) δ 178.5, 159.5, 157.7, 141.2, 136.8, 136.7, 134.1, 128.0, 124.8, 122.4, 121.7, 121.6, 114.4, 109.7, 107.0, 106.8, 97.5, 97.3, 52.3.

3-hydroxy-3-(1H-indol-3-yl)indolin-2-one⁸³: 80%, (R_f = 0.40, 50:50 EtOAc/Hex), ¹H NMR (DMSO- d_6 , 500 MHz) δ 10.98 (s, 1H), 10.34 (s, 1H), 7.33 (t, 2H, J = 8.2 Hz), 7.26-7.22 (m, 2H), 7.06 (d, 1H, J = 2.7 Hz), 7.02 (dt, 1H, J = 1.4 Hz & 6.8 Hz), 6.94 (t, 1H, J = 6.9 Hz), 6.90-6.84 (m, 2H), 6.35 (s,

1H); ^{13}C NMR (DMSO- d_6 , 125 MHz) δ 179.0, 142.2, 137.3, 133.9, 129.6, 125.4, 125.3, 124.0, 122.2, 121.5, 120.8, 119.0, 115.9, 112.0, 110.1, 75.4.

3-(5-methoxy-1H-indol-3-yl)indolin-3-ol^{83, 84}: 82%, (R_f = 0.40, 30:70 EtOAc/Hex), ^1H NMR (DMSO- d_6 , 500 MHz) δ 10.91 (s, 1H), 10.52 (s, 1H), 7.34-7.30 (m, 2H), 7.23 (d, 1H, J = 8.9 Hz), 7.11 (d, 1H, J = 2.0 Hz), 7.03 (t, 1H, J = 6.9 Hz), 6.92 (d, 1H, J = 7.6 Hz), 6.82 (d, 1H, J = 2.7 Hz), 6.72 (dd, 1H, J = 2.0 Hz & 6.2 Hz), 3.67 (s, 3H); ^{13}C NMR (DMSO- d_6 , 125 MHz) δ 176.1, 152.8, 142.2, 132.0, 129.7, 129.0, 125.6, 125.2, 124.8, 121.9, 112.5, 112.1, 111.5, 110.0, 103.1, 80.7, 55.1.

5-bromo-3-hydroxy-3-(1H-indol-3-yl)indolin-2-one⁸³: 78%, (R_f = 0.50, 50:50 EtOAc/Hex), ^1H NMR (DMSO- d_6 , 500 MHz) δ 11.05 (s, 1H), 10.5 (s, 1H), 7.44-7.42 (m, 1H), 7.34 (d, 2H, J = 8.9 Hz), 7.30 (d, 1H, J = 2.1 Hz), 7.10 (d, 1H, J = 2.0 Hz), 7.04 (t, 1H, J = 8.2 Hz), 6.90-6.86 (m, 2H), 6.53 (s, 1H); ^{13}C NMR (DMSO- d_6 , 125 MHz) δ 177.9, 136.8, 135.9, 131.7, 127.3, 124.7, 123.6, 121.2, 120.0, 118.7, 114.6, 113.3, 111.8, 111.6, 74.9.

3-(2-nitroethyl)-1H-indole⁸⁵: 81%, (R_f = 0.50, 20:80 EtOAc/Hex), ^1H NMR (CDCl_3 , 500 MHz) δ 8.04 (brs, 1H), 7.56 (d, 1H, J = 7.6 Hz), 7.35 (d, 1H, J = 8.2 Hz), 7.21 (t, 1H, J = 7.6 Hz), 7.15 (t, 1H, J = 8.2 Hz), 7.01 (d, 1H, J = 2.7 Hz), 4.64 (t, 2H, J = 6.8 Hz), 3.47 (t, 2H, J = 6.8 Hz); ^{13}C NMR (CDCl_3 , 125 MHz) δ 136.1, 126.5, 122.5, 122.4, 119.8, 118.0, 111.4, 109.8, 75.6, 23.5.

2-(1H-indol-3-yl)ethanamine⁸⁶: 81%, (R_f = 0.50, 10:90 DCM/MeOH), ^1H NMR (CDCl_3 , 500 MHz) δ 8.31 (brs, 1H), 7.61 (d, 1H, J = 8.2 Hz), 7.35 (d, 1H, J = 8.2 Hz), 7.19 (t, 1H, J = 8.2 Hz), 7.11 (t, 1H, J = 8.2 Hz), 7.01 (d, 1H, J = 2.0 Hz), 3.04 (t, 2H, J = 6.8 Hz), 2.91 (t, 2H, J = 6.8 Hz), 1.25 (brs, 2H); ^{13}C NMR (CDCl_3 , 125 MHz) δ 136.4, 127.4, 122.5, 121.9, 119.2, 118.8, 113.6, 111.1, 42.3, 29.5.

1-phenyl-2,3,4,9-tetrahydro-1H-pyrido[3,4-b]indole^{87, 88}: 72%, (R_f = 0.50, 70:30 EtOAc/Hex), ^1H NMR (DMSO- d_6 , 500 MHz) δ 10.42 (s, 1H), 7.40 (d, 1H, J = 7.5 Hz), 7.34-7.27 (m, 5H), 7.21 (d, 1H, J = 8.2 Hz), 7.01-6.92 (m, 2H), 5.07 (s, 1H), 3.07-3.02 (m, 1H), 2.95- 2.90 (m, 1H), 2.83 (brs, 1H), 2.75- 2.70 (m, 1H), 2.68- 2.63 (m, 1H); ^{13}C NMR (DMSO- d_6 , 125 MHz) δ 143.2, 135.9, 135.4, 128.5, 128.1, 127.2, 126.8, 120.5, 118.2, 117.5, 111.0, 108.2, 56.6, 41.2, 22.2.

Supporting Information

Green chemistry matrix calculations, crystallographic data for **3mn**, water contact angle of MoS₂, GCN and MoS₂-GCN (1:1) nanocomposite, and ¹H & ¹³C NMR data of the synthesized compounds.

Acknowledgements

Advanced Materials Research Center (AMRC), Indian Institute of Technology Mandi is gratefully acknowledged for providing all of the necessary laboratory and instrumentation facilities. VK acknowledges the financial support from the Department of Science and Technology, India, under Young Scientist Scheme (YSS/2014/000456). AB and SK acknowledge CSIR, India and UGC India, for senior research fellowships, respectively. TC thanks MHRD India, for the junior research fellowship.

References

- [1] E. Pérez-Mayoral, V. Calvino-Casilda, E. Soriano *Catalysis Science & Technology*. **2016**, *6*, 1265-1291.
- [2] A. Corma, L. T. Nemeth, M. Renz, S. Valencia *Nature*. **2001**, *412*, 423-425.
- [3] J. Kang, K. Cheng, L. Zhang, Q. Zhang, J. Ding, W. Hua, Y. Lou, Q. Zhai, Y. Wang *Angewandte Chemie*. **2011**, *123*, 5306-5309.
- [4] Y. Zhang, A. Wang, T. Zhang *Chemical Communications*. **2010**, *46*, 862-864.
- [5] R. L. Espinoza, K. Jothimurugesan, K. L. Coy, J. D. Ortego Jr, N. Srinivasan, O. P. Ionkina in Silica-alumina catalyst support, catalysts made therefrom and methods of making and using same, Vol. (Ed.^Eds.: Editor), Google Patents, City, **2009**.
- [6] C. M. Crudden, M. Sateesh, R. Lewis *Journal of the American Chemical Society*. **2005**, *127*, 10045-10050.
- [7] F. Su, J. Zeng, X. Bao, Y. Yu, J. Y. Lee, X. Zhao *Chemistry of materials*. **2005**, *17*, 3960-3967.
- [8] P. V. Shanahan, L. Xu, C. Liang, M. Waje, S. Dai, Y. Yan *Journal of Power Sources*. **2008**, *185*, 423-427.

- [9] Y. Li, W.-N. Wang, Z. Zhan, M.-H. Woo, C.-Y. Wu, P. Biswas *Applied Catalysis B: Environmental*. **2010**, *100*, 386-392.
- [10] G. G. Wildgoose, C. E. Banks, R. G. Compton *Small*. **2006**, *2*, 182-193.
- [11] P. V. Kamat *The Journal of Physical Chemistry Letters*. **2009**, *1*, 520-527.
- [12] P. Serp, M. Corrias, P. Kalck *Applied Catalysis A: General*. **2003**, *253*, 337-358.
- [13] A. S. Aricò, P. Bruce, B. Scrosati, J.-M. Tarascon, W. Van Schalkwijk *Nature materials*. **2005**, *4*, 366-377.
- [14] L. Yin, J. Liebscher *Chemical Reviews*. **2007**, *107*, 133-173.
- [15] E. Negishi, A. O. King, N. Okukado *The Journal of Organic Chemistry*. **1977**, *42*, 1821-1823.
- [16] P. M. Ajayan, O. Z. Zhou in *Applications of carbon nanotubes, Vol.*, Springer, **2001**, pp.391-425.
- [17] R. H. Baughman, A. A. Zakhidov, W. A. De Heer *Science*. **2002**, *297*, 787-792.
- [18] B. Vigolo, A. Penicaud, C. Coulon, C. Sauder, R. Pailier, C. Journet, P. Bernier, P. Poulin *Science*. **2000**, *290*, 1331-1334.
- [19] J. Peng, W. Gao, B. K. Gupta, Z. Liu, R. Romero-Aburto, L. Ge, L. Song, L. B. Alemany, X. Zhan, G. Gao *Nano letters*. **2012**, *12*, 844-849.
- [20] C. Moreno-Castilla, F. Maldonado-Hódar *Carbon*. **2005**, *43*, 455-465.
- [21] B. F. Machado, P. Serp *Catalysis Science & Technology*. **2012**, *2*, 54-75.
- [22] X.-K. Kong, C.-L. Chen, Q.-W. Chen *Chemical Society Reviews*. **2014**, *43*, 2841-2857.
- [23] A. Thomas, A. Fischer, F. Goettmann, M. Antonietti, J.-O. Müller, R. Schlögl, J. M. Carlsson *Journal of Materials Chemistry*. **2008**, *18*, 4893-4908.
- [24] J. Zhu, P. Xiao, H. Li, S. n. A. Carabineiro *ACS applied materials & interfaces*. **2014**, *6*, 16449-16465.
- [25] H. Jüntgen *Fuel*. **1986**, *65*, 1436-1446.
- [26] H. Jüntgen *ChemInform*. **1987**, *18*.
- [27] M. L. Studebaker *Rubber Chemistry and Technology*. **1957**, *30*, 1400-1483.
- [28] J. Wang, G. Yin, Y. Shao, S. Zhang, Z. Wang, Y. Gao *Journal of Power Sources*. **2007**, *171*, 331-339.

- [29] R. J. White, R. Luque, V. L. Budarin, J. H. Clark, D. J. Macquarrie *Chemical Society Reviews*. **2009**, *38*, 481-494.
- [30] D. R. Dreyer, C. W. Bielawski *Chemical Science*. **2011**, *2*, 1233-1240.
- [31] A. Bahuguna, S. Kumar, V. Krishnan *ChemistrySelect*. **2018**, *3*, 12373-12379.
- [32] V. Polshettiwar, R. S. Varma *Green Chemistry*. **2010**, *12*, 743-754.
- [33] L. L. Chng, N. Erathodiyil, J. Y. Ying *Accounts of chemical research*. **2013**, *46*, 1825-1837.
- [34] Y. Zhu, L. P. Stubbs, F. Ho, R. Liu, C. P. Ship, J. A. Maguire, N. S. Hosmane *ChemCatChem*. **2010**, *2*, 365-374.
- [35] M. Chhowalla, H. S. Shin, G. Eda, L.-J. Li, K. P. Loh, H. Zhang *Nature chemistry*. **2013**, *5*, 263-275.
- [36] C. Tan, H. Zhang *Chemical Society Reviews*. **2015**, *44*, 2713-2731.
- [37] Y. Wang, H. Li, J. Yao, X. Wang, M. Antonietti *Chemical Science*. **2011**, *2*, 446-450.
- [38] Y. Gong, M. Li, H. Li, Y. Wang *Green Chemistry*. **2015**, *17*, 715-736.
- [39] F. Goettmann, A. Fischer, M. Antonietti, A. Thomas *Angewandte Chemie International Edition*. **2006**, *45*, 4467-4471.
- [40] X. Li, Y. Wang, L. Kang, M. Zhu, B. Dai *Journal of catalysis*. **2014**, *311*, 288-294.
- [41] F. Su, M. Antonietti, X. Wang *Catalysis Science & Technology*. **2012**, *2*, 1005-1009.
- [42] F. Goettmann, A. Fischer, M. Antonietti, A. Thomas *New Journal of chemistry*. **2007**, *31*, 1455-1460.
- [43] S. Dadashi-Silab, B. Kiskan, M. Antonietti, Y. Yagci *Rsc Advances*. **2014**, *4*, 52170-52173.
- [44] M. Zhang, Y.-H. Liu, Z.-R. Shang, H.-C. Hu, Z.-H. Zhang *Catalysis Communications*. **2017**, *88*, 39-44.
- [45] L. Wang, C. Wang, W. Liu, Q. Chen, M. He *Tetrahedron Letters*. **2016**, *57*, 1771-1774.
- [46] A. Bahuguna, S. Kumar, V. Sharma, K. L. Reddy, K. Bhattacharyya, P. C. Ravikumar, V. Krishnan *ACS Sustainable Chemistry & Engineering*. **2017**, *5*, 8551-8567.
- [47] K. Sridharan, E. Jang, T. J. Park *Applied Catalysis B: Environmental*. **2013**, *142*, 718-728.
- [48] J. Ran, J. Yu, M. Jaroniec *Green Chemistry*. **2011**, *13*, 2708-2713.
- [49] S. E. O'Connor, J. J. Maresh *Natural product reports*. **2006**, *23*, 532-547.
- [50] A. Bahuguna, R. Sharma, P. Sagara, P. Ravikumar *Synlett*. **2017**, *28*, 117-121.

- [51] K. Patel, M. Gadewar, R. Tripathi, S. Prasad, D. K. Patel *Asian Pacific journal of tropical biomedicine*. **2012**, *2*, 660-664.
- [52] Y. Oikawa, H. Hirasawa, O. Yonemitsu *Tetrahedron Letters*. **1978**, *19*, 1759-1762.
- [53] M. Li, A. Taheri, M. Liu, S. Sun, Y. Gu *Advanced Synthesis & Catalysis*. **2014**, *356*, 537-556.
- [54] U. C. Rajesh, J. Wang, S. Prescott, T. Tsuzuki, D. S. Rawat *ACS Sustainable Chemistry & Engineering*. **2014**, *3*, 9-18.
- [55] S. Kumar, N. L. Reddy, A. Kumar, M. V. Shankar, V. Krishnan *International Journal of Hydrogen Energy*. **2017**.
- [56] S. Kumar, V. Sharma, K. Bhattacharyya, V. Krishnan *Materials Chemistry Frontiers*. **2017**, *1*, 1093-1106.
- [57] J. Zhao, Z. Zhang, S. Yang, H. Zheng, Y. Li *Journal of Alloys and Compounds*. **2013**, *559*, 87-91.
- [58] P. Drabina, B. Brož, Z. Padělková, M. Sedlák *Journal of Organometallic Chemistry*. **2011**, *696*, 971-981.
- [59] G. Huang, H. Sun, X. Qiu, Y. Shen, J. Jiang, L. Wang *Journal of Organometallic Chemistry*. **2011**, *696*, 2949-2957.
- [60] M. Jeganathan, K. Kanagaraj, A. Dhakshinamoorthy, K. Pitchumani *Tetrahedron Letters*. **2014**, *55*, 2061-2064.
- [61] C. Zhu, Q. Mao, C. Li, Y. Zhou, X. Wu, Y. Luo, Y. Li *Catalysis Communications*. **2018**, *104*, 123-127.
- [62] X. Zhang, Z. Zhang, J. Boissonault, S. M. Cohen *Chemical Communications*. **2016**, *52*, 8585-8588.
- [63] A. Izaga, R. P. Herrera, M. C. Gimeno *ChemCatChem*. **2017**, *9*, 1313-1321.
- [64] B. Das, N. Chowdhury, K. Damodar, K. R. Reddy *Helvetica chimica acta*. **2007**, *90*, 340-345.
- [65] G. Bartoli, M. Bosco, S. Giuli, A. Giuliani, L. Lucarelli, E. Marcantoni, L. Sambri, E. Torregiani *The Journal of organic chemistry*. **2005**, *70*, 1941-1944.
- [66] S. Sobhani, R. Jahanshahi *New Journal of Chemistry*. **2013**, *37*, 1009-1015.
- [67] X.-Q. Hao, Y.-X. Xu, M.-J. Yang, L. Wang, J.-L. Niu, J.-F. Gong, M.-P. Song *Organometallics*. **2012**, *31*, 835-846.

- [68] M. L. Kantam, S. Laha, J. Yadav, P. Srinivas *Synthetic Communications*[®]. **2009**, *39*, 4100-4108.
- [69] J. S. Yadav, B. V. SubbaReddy, K. U. Gayathri, S. Meraj, A. R. Prasad *Synthesis*. **2006**, *2006*, 4121-4123.
- [70] J. Azizian, A. A. Mohammadi, N. Karimi, M. R. Mohammadizadeh, A. R. Karimi *Catalysis Communications*. **2006**, *7*, 752-755.
- [71] K. Chang, Z. Mei, T. Wang, Q. Kang, S. Ouyang, J. Ye *ACS nano*. **2014**, *8*, 7078-7087.
- [72] M. Wen, T. Xiong, Z. Zang, W. Wei, X. Tang, F. Dong *Optics express*. **2016**, *24*, 10205-10212.
- [73] R. P. Herrera, V. Sgarzani, L. Bernardi, A. Ricci *Angewandte Chemie International Edition*. **2005**, *44*, 6576-6579.
- [74] W. Zhuang, R. G. Hazell, K. A. Jørgensen *Organic & biomolecular chemistry*. **2005**, *3*, 2566-2571.
- [75] Y.-X. Jia, S.-F. Zhu, Y. Yang, Q.-L. Zhou *The Journal of organic chemistry*. **2006**, *71*, 75-80.
- [76] S.-F. Lu, D.-M. Du, J. Xu *Organic letters*. **2006**, *8*, 2115-2118.
- [77] P. Kumar, S. Lympelopoulou, K. Griffiths, S. I. Sampani, G. E. Kostakis *Catalysts*. **2016**, *6*, 140.
- [78] P. K. Singh, A. Bisai, V. K. Singh *Tetrahedron letters*. **2007**, *48*, 1127-1129.
- [79] S.-Y. Wang, S.-J. Ji *Tetrahedron*. **2006**, *62*, 1527-1535.
- [80] A. Kamal, Y. Srikanth, M. N. A. Khan, T. B. Shaik, M. Ashraf *Bioorganic & medicinal chemistry letters*. **2010**, *20*, 5229-5231.
- [81] P. Paira, A. Hazra, S. Kumar, R. Paira, K. B. Sahu, S. Naskar, S. Mondal, A. Maity, S. Banerjee, N. B. Mondal *Bioorganic & medicinal chemistry letters*. **2009**, *19*, 4786-4789.
- [82] G. Brahmachari, B. Banerjee *ACS Sustainable Chemistry & Engineering*. **2014**, *2*, 2802-2812.
- [83] P. Chauhan, S. S. Chimni *Chemistry-A European Journal*. **2010**, *16*, 7709-7713.
- [84] J. Deng, S. Zhang, P. Ding, H. Jiang, W. Wang, J. Li *Advanced Synthesis & Catalysis*. **2010**, *352*, 833-838.
- [85] Q. V. Vo, C. Trenerry, S. Rochfort, J. Wadeson, C. Leyton, A. B. Hughes *Bioorganic & medicinal chemistry*. **2014**, *22*, 856-864.

- [86] K. Nicolaou, A. Krasovskiy, U. Majumder, V. E. Trépanier, D. Y.-K. Chen *Journal of the American Chemical Society*. **2009**, *131*, 3690-3699.
- [87] M. Desroses, T. Koolmeister, S. Jacques, S. Llona-Minguez, M.-C. Jacques-Cordonnier, A. Cázares-Körner, T. Helleday, M. Scobie *Tetrahedron Letters*. **2013**, *54*, 3554-3557.
- [88] N. Srinivasan, A. Ganesan *Chemical Communications*. **2003**, 916-917.